

Short communication

Further evidence of unstable reverse polarity geomagnetic field across the Olduvai subchron: paleomagnetic and multispecimen paleointensity study on Khertvisi lava flows (Lesser Caucasus)

Avto Goguitchaichvili^{a,*}, Juan Morales^a, Goga Vashakidze^b, Manuel Calvo-Rathert^c, Vladimir A. Lebedev^d, Vadim Kravchinsky^e, Miguel Cervantes-Solano^a, Daniel Sebastián Reyes^a

^a Laboratorio Interinstitucional de Magnetismo Natural, Instituto de Geofísica, UNAM – Campus Morelia, México

^b I. Javakishvili Tbilisi State University, Tbilisi, Georgia

^c Departamento de Física, EPS Campus Rio Vena – Universidad de Burgos, 09006 Burgos, Spain

^d Institute of Geology of Ore Deposits, Petrography, Mineralogy and Geochemistry, Russian Academy of Sciences (IGEM RAS), Moscow, Russia

^e Geophysics, Department of Physics, University of Alberta, Edmonton, Alberta T6G2E1, Canada

ARTICLE INFO

Keywords:

Paleomagnetism

Multi-specimen paleointensity

Olduvai

Caucasus

ABSTRACT

Goguitchaichvili et al. (Physics of the Earth and Planetary Interiors, doi.org/10.1016/j.pepi.2020.106641, 2021) reported a detailed rock-magnetic and paleointensity study of a Lesser Caucasus lava sequence comprised between 1.93 ± 0.09 and 1.78 ± 0.11 Ma. Reverse polarity magnetization determined for 20 consecutive lava flows permitted to suggest that the Olduvai subchron is probably disrupted by a short reverse-polarity episode. No paleointensity was obtained because of thermally unstable samples. Here, we report a detailed rock-magnetic, paleomagnetic, and multispecimen parallel differential pTRM absolute paleointensities performed on the nearby parallel Khertvisi lava succession. New isotopic age determinations indicate that the lavas of the Khertvisi section erupted in the Early Pleistocene, at the boundary of Gelasian and Calabrian ages in a time span of 1.88 ± 0.10 to 1.71 ± 0.12 Ma. All lava flows yielded well-defined reverse polarity magnetization with site mean directions $\text{Inc.} = -56.1^\circ$, $\text{Dec} = 189.5^\circ$, $N = 20$ (lava flows), $\alpha_{95} = 2.3^\circ$, $k = 187$. These directions are close to the Toloshi mean paleodirections, and both slightly deviate clockwise from the geocentric axial dipole and expected Plio-Quaternary directions. The values of the virtual geomagnetic pole (VGP) scatter parameters indicate that the studied sequence was formed during a very short time, most probably insufficient to average paleosecular variation. The multispecimen methodology provided a relatively low paleointensity for most analyzed lava flows, comparable to the transitional field intensity in Georgia during the Brunhes and Matuyama chrons. These results definitively confirm a rather unstable, reverse polarity geomagnetic field regime across the Olduvai normal superchron. Thus, we propose to consider the Khertvisi section as the firm, volcanic evidence of Olduvai's short-lived geomagnetic event.

1. Introduction

Geomagnetic polarity chrons, time intervals on the order of 10^5 years or so, were first defined by Cox et al. (1963). The evolution of precise isotopic datings led to detect several subchrons as well, being Jaramillo, Olduvai, and Reunion (Cox and Dalrymple, 1967, see also Opdyke and Channell, 1996) the most representative events. Singer et al. (1999), Singer and Brown (2002), Singer and Laurie (2004), Singer et al. (2005)

developed a Geomagnetic Instability Time Scale (GITS) for the Matuyama reversed and Brunhes normal Chrons where the Olduvai normal polarity subchron is comprised between 1922 ± 66 and 1775 ± 15 ka. Based on relative paleointensity composite records from sediment cored at Ocean Drilling Program sites 983 and 984, Channell et al. (2002) locate the Olduvai from 1945 to 1778 ka.

Still, the precise estimation of the top and base of the Olduvai subchron is a matter of debate (Channell et al., 2020). After Shackleton et al.

* Corresponding author at: Sabbatical at Geophysics, Department of Physics, University of Alberta, Edmonton, Alberta, Canada T6G2E1.

E-mail address: avto@geofisica.unam.mx (A. Goguitchaichvili).

<https://doi.org/10.1016/j.pepi.2022.106952>

Received 28 April 2022; Received in revised form 27 September 2022; Accepted 30 September 2022

Available online 4 October 2022

0031-9201/© 2022 Elsevier B.V. All rights reserved.

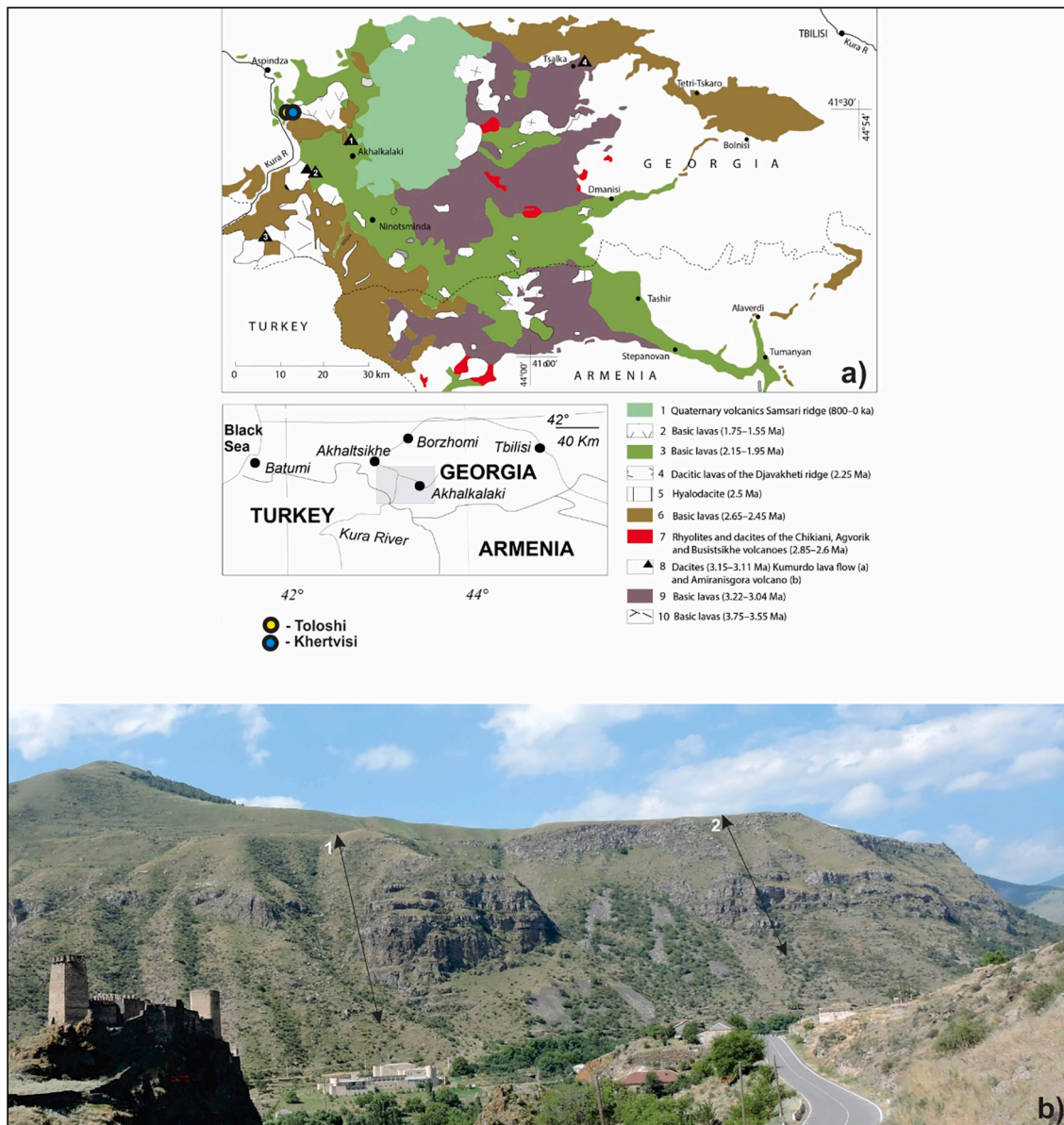


Fig. 1. Schematic geological map of the Pliocene-Pleistocene magmatism in the Javakheti Highland showing the location of the Toloshi (1) and Khertvisi (2) sections (modified after Lebedev et al., 2008). Paleomagnetic data from Toloshi profile are reported in Goguitchaichvili et al., 2021 while Khertvisi lava succession denote to present study (see text for more details).

1 - Late Quaternary volcanic rocks (andesites and dacites) of the Samsari ridge (<800 ka); 2–10 Pliocene – Early Quaternary volcanic rocks of the Akhalkalaki Formation (2 - basic lavas 1.75–1.50 Ma, 3 - basic lavas 2.15–1.95 Ma, 4 - later dacites and rhyolites of the Javakheti ridge 2.25 Ma, 5 - hyalodacite 2.5 Ma, 6 - basic lavas 2.65–2.45 Ma, 7 - earlier rhyolites and dacites of the Javakheti ridge 2.85–2.6 Ma, 8 - dacites of the SW part of the Javakheti highland 3.15–3.11 Ma, 9 - basic lavas 3.22–3.04 Ma, 10 - basic lavas 3.75–3.55 Ma). Also shown is a simplified stratigraphic diagram showing the thicknesses of 20 consecutive lava flows.

(1990), the base of Olduvai corresponds to an age of 1950 ka. The same conclusion was reached by Hilgen in 1991 (see also Lourens et al., 1996 and Ogg, 2012). Lisiecki and Raymo (2005) suggested the base of Olduvai at 1968 ka, while Rivera et al. (2017) place it at 1948 ± 2 ka based on an $^{40}\text{Ar}/^{39}\text{Ar}$ age determination. As far as the uppermost Olduvai age is concerned, the most comprehensive study belongs to Singer (2014), suggesting an age of 1787 ± 15 ka for the top of the Olduvai based on isotopic dates.

There is a general agreement among the paleomagnetic community that the Olduvai subchron is characterized by normal polarity magnetization. Numerous studies showed, however, that the whole subchron is probably not uniform. Intermediate polarity lava flows were reported by Singer and Laurie (2004), while Tric et al. (1991) found a transitional field in marine sediments. A short inverted polarity, within the Olduvai

event, was reported by Zijdeveld et al. (1991), Yang et al. (2008), and Kusu et al. (2016). Goguitchaichvili et al. (2021) reported a detailed rock-magnetic and paleomagnetic study of the Lesser Caucasus lava sequence at Toloshi, comprised between 1.93 ± 0.09 and 1.78 ± 0.11 Ma. All twenty lava flows yielded clearly defined reverse polarity magnetization interpreted as a relatively short geomagnetic event within the normal-polarity Olduvai subchron. Because of the importance of these findings, additional samples were collected from a nearby, parallel Khertvisi section comprised of 21 consecutive lava flows. Both, new isotopic ages and paleomagnetic results were obtained. In addition, multi-specimen absolute intensity determinations were successfully determined for five independent cooling units.

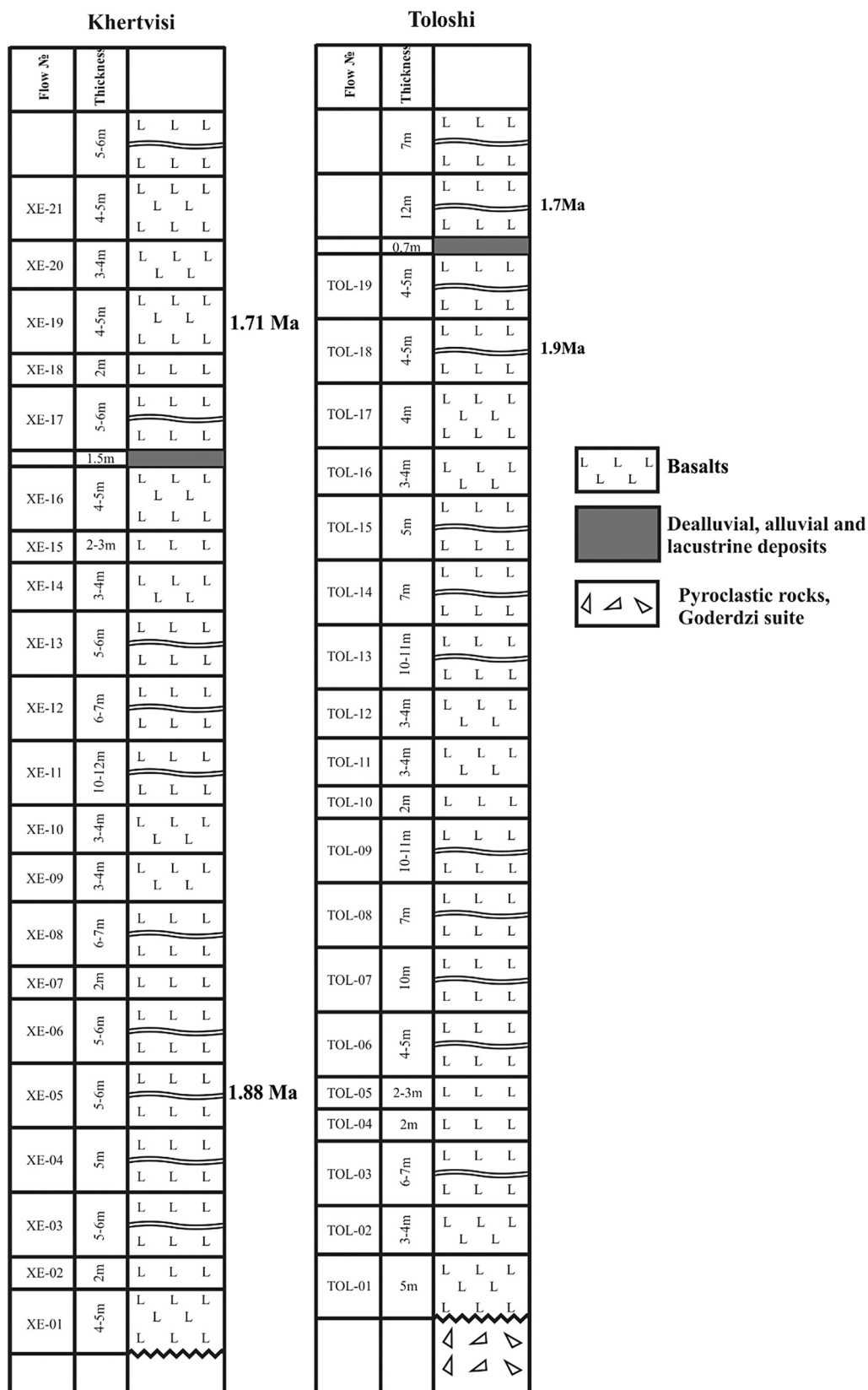


Fig. 2. A simplified stratigraphical column for Khertvisi and Toloshi sections. See text for more details.

Table 1

Isotopic age determinations for two Khertvisi lava flows. Please see text for technical details.

| Lab Code | Rock type | Object | K, % $\pm \sigma$ | $^{40}\text{Ar}^*$ $\pm \sigma$ | $^{40}\text{Ar}_{\text{atm}}$, % (in sample) | Age, Ma $\pm 2\sigma$ |
|----------|-----------|-----------------------|-------------------|---------------------------------|---|-----------------------|
| XE-19 | Basalt | Khertvisi, Upper Part | 0.77 \pm 0.015 | 0.091 \pm 0.002 | 59.5 | 1.71 \pm 0.10 |
| XE-05 | Basalt | Khertvisi, Lower Part | 0.95 \pm 0.015 | 0.124 \pm 0.003 | 91.6 | 1.88 \pm 0.12 |

2. Sampling details and isotopic dating

The studied area belongs to the Javakheti Highland, characterized by an extremely intense Pliocene-Quaternary volcanic activity in the northwestern sector of the Lesser Caucasus (Fig. 1a). Some details concerning regional geology and the evolution of young magmatism were discussed (Lebedev et al., 2008, 2019). A brief geological description of the studied area (northwestern part of Javakheti Highland near the confluence of rivers Mtkvari and Paravani is given in Goguitchaichvili et al. (2021). In this study, we sampled a Khertvisi lava sequence, which represents a parallel section (Fig. 1b) to the previously analyzed Toloshi sequence (Goguitchaichvili et al., 2021). Both sites are located on the left bank of the Mtkvari (Kura) River (Fig. 2). The Khertvisi sequence comprises twenty-one lava flows of calc-alkaline basalts (SiO_2 –48.7–50.7, $\text{Na}_2\text{O} + \text{K}_2\text{O}$ – 4.7, K_2O – 1.0–1.1 wt%) with variable thicknesses from about 2 to 10 m. A 1.5 m thick reddish sedimentary layer is detected between lava flows XE16 and XE17. The same layer is only half thick in the Toloshi section. In any case, the existence of such a unit reflects some kind of interruption of lava emission dynamics. At

least eight standard paleomagnetic cores were collected and oriented with both magnetic and sun compasses in each flow. In a few cases, the solar orientation was impossible, and the local declination value was used as a correction factor. No tectonic correction was applied since no significant or measurable dip was observed during the fieldwork.

New radiometric ages obtained in this study were performed in the Institute of Geology of Ore Deposits, Petrography, Mineralogy, and Geochemistry – Russian Academy of Sciences. The methodology is the same as the one used in Goguitchaichvili et al. (2021). The microlithic groundmass of lavas separated from phenocrysts was used for the dating. The analyses of radiogenic ^{40}Ar content were carried out on the high-sensitive low-blank mass spectrometer MI-1201 IG (SEMI) (Lebedev et al., 2010). The isotopic dilution technique with monoisotopic ^{38}Ar as spike was used. Correctness of measurements was controlled by repeating analyses of the international standard samples MMhb-1, Bern-4 M, muscovite P-207, and argon with atmospheric composition. The total blank of ^{40}Ar in analyses did not exceed 0.003 ng. The potassium content of the samples was determined by the flame photometry method using an FPA-01 spectrometer (ELAM Center). The total uncertainties of K-Ar dating ($\pm 2\sigma$) are given in Table 1, together with age values. The calculations were based on the international values of decay constants for radioactive isotopes (Steiger and Jäger, 1977).

3. Magnetic measurements

Continuous thermomagnetic curves (susceptibility vs. temperature) were recorded up to 600 °C using an AGICO MFK1a Kappabridge with a heating (and cooling) rate held to 15 °C per minute. The experiments were performed in argon to avoid potential magneto-chemical changes. These measurements (Fig. 3) are useful to estimate the thermal stability

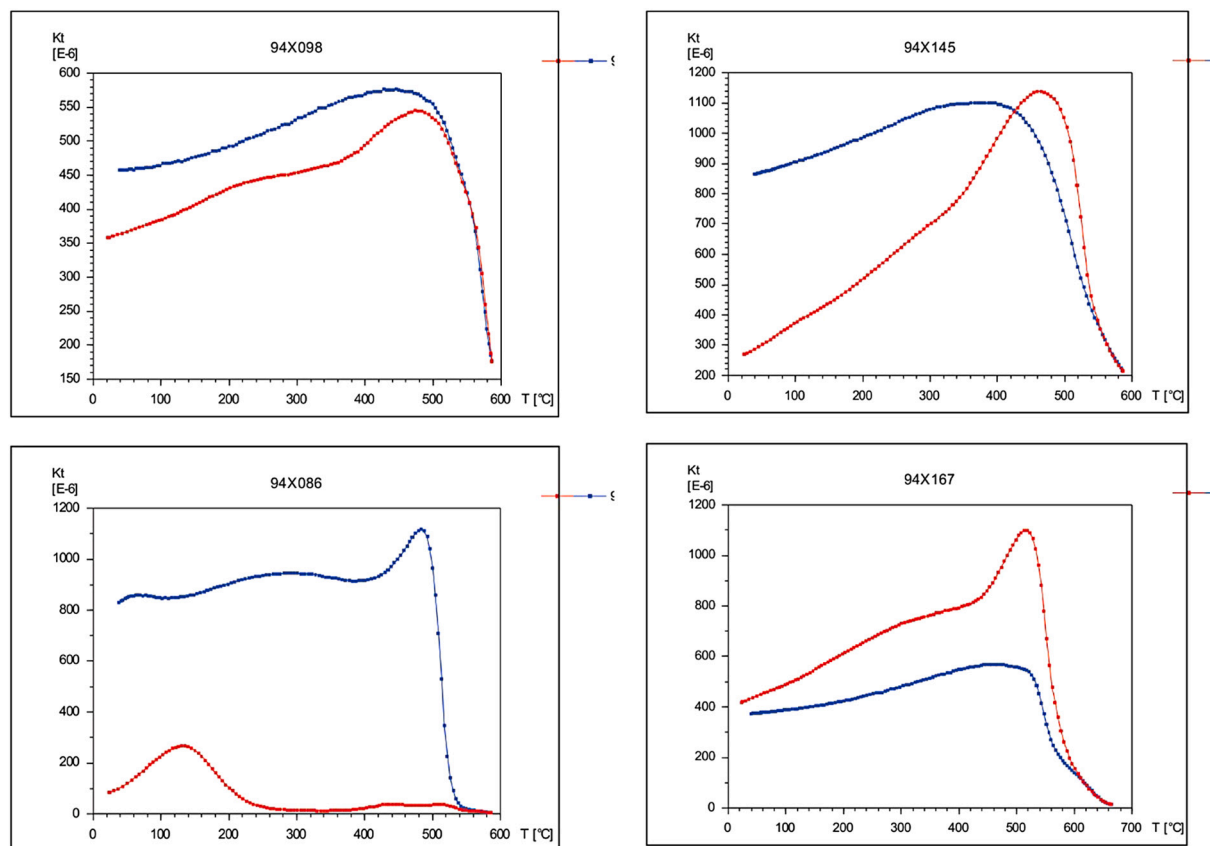


Fig. 3. Representative examples of magnetic susceptibility vs. temperature curves. The red and blue lines indicate the behavior during heating and cooling respectively, the relative susceptibility is shown in arbitrary units. (For interpretation of the references to colour in this figure legend, the reader is referred to the web version of this article.)

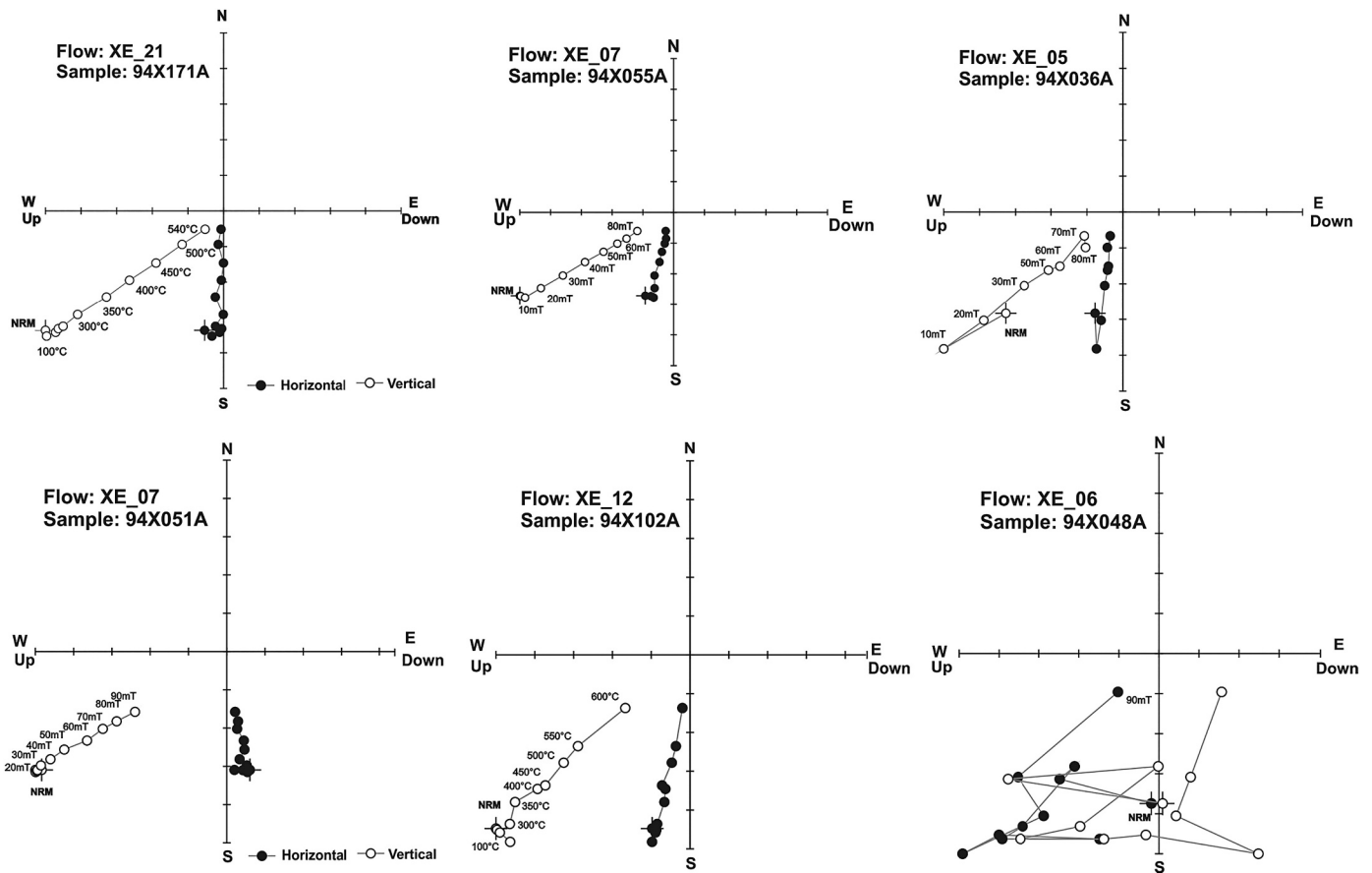


Fig. 4. Orthogonal demagnetization vector plots for representative samples. The numbers refer to the peak values of alternating fields expressed in mT or degrees Celsius for the maximum temperature value step.

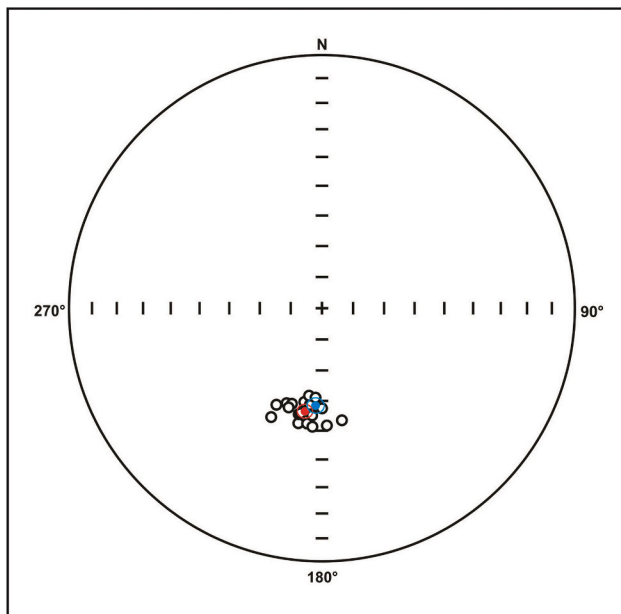


Fig. 5. Flow-mean characteristic paleodirections for the Khertvisi lava flows. The red circle is the mean direction and his 95% confidence for this study, circle in blue is the direction retrieved from APTW for Eurasia for the last 5 Ma (Besse and Courtillot, 2002). (For interpretation of the references to colour in this figure legend, the reader is referred to the web version of this article.)

of samples, and therefore their suitability for paleointensity

determinations, as well as to reveal magnetic carriers through the determination of their Curie points.

To determine flow-mean paleodirections (Fig. 4 and 5), eight specimens per flow, on average, were subjected to either alternating field demagnetization using an LDA-3 AGICO demagnetizer up to 90 mT, or thermal treatments until 600 °C (Fig. 4) using an MMTD80 device. At least six aligned steps pointing to the origin were used to calculate inclination and declination at the sample level, with values of maximum angular deviation less than 3°. The remanence components were determined using the principal component analysis method (Kirschvink, 1980), while the determination of flow-mean paleodirections was based on the Fisher statistics (Fisher, 1953).

Absolute paleointensity determinations were carried out with the multispecimen parallel differential pTRM method (Dekkers and Bönnel, 2006), including the protocols for fraction and domain-state corrections (FC, DSC, respectively) (Fabian and Leonhardt, 2010), hereafter referred as MSP. The specimen preparation for the MSP was as follows: One standard paleomagnetic core per flow was cut into two disc-shaped halves; each of them was further split into pie-slices-shaped quarters, obtaining eight sub-specimens in total. Each sub-specimen was pressed into a salt pellet with standard paleomagnetic dimensions. Based on AF demagnetization plots of pilot specimens, which revealed the presence of small secondary imprints, a 5 mT demagnetization was applied to the sub-specimens before applying the MSP in order to eliminate possible viscous overprints.

The MSP experimental protocol (Fig. 6) consisted of the sequence of the following steps: (a) measurement of the NRM vector; (b) using a special ten-position sample holder, specimens were oriented in such a way that the NRM directions of each sub-specimen lay parallel to the heating chamber axis; subsequently they were heated at the

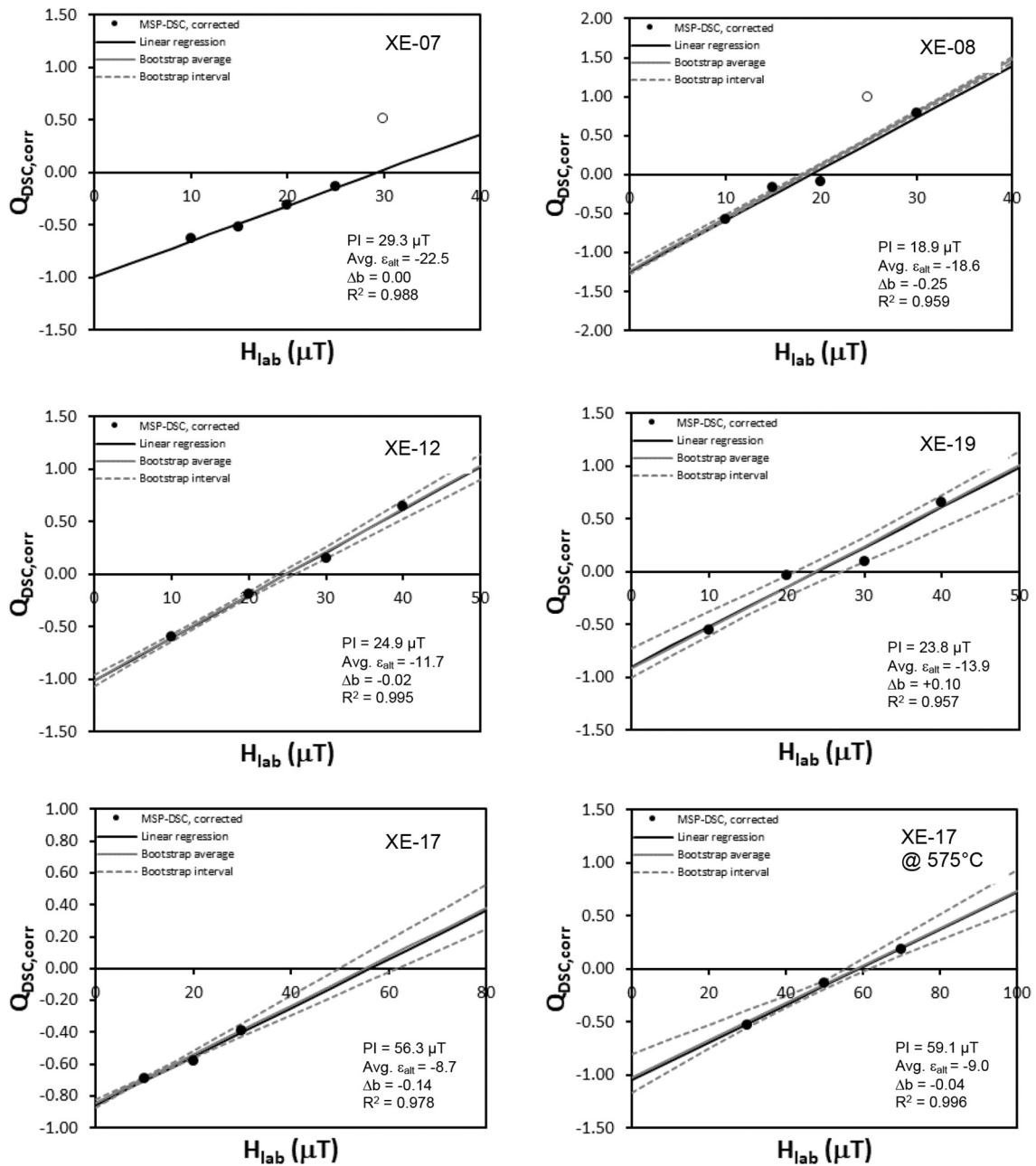


Fig. 6. Representative examples of multi-specimen absolute intensity determinations using the MSP-VBA Tool (Monster et al., 2015). 475 °C was used for all samples to produce partial thermoremanences except flow XE-17, which was additionally subjected to 525 °C. Please see the text for more details.

corresponding temperature in an axial laboratory field and therefore parallel to the remanence of the specimens (see below); (c) specimens were set and heated as in the previous step but in an anti-parallel field; (d) specimens were heated in zero-field and cooled in a parallel laboratory field; (e) step (b) was repeated. After each of the steps (b) to (e), the acquired magnetization was measured using an AGICO JR6 spinner magnetometer. As stated by Monster et al. (2015), the QDB ratio (Dekkers and Böhnel, 2006) is defined as follows:

$$Q_{DB} = \frac{m_1 - m_0}{m_0}$$

where m_0 and m_1 are the scalar intensities of the two remanences. The fraction-corrected (MSP-FC) and domain-state corrected (MSP-DSC) ratios (both defined in Fabian and Leonhardt, 2010) are:

$$Q_{FC} = 2 \frac{m_1 - m_0}{2m_0 - m_1 - m_2}$$

$$Q_{DSC} = 2 \frac{(1 + \alpha)m_1 - m_0 - \alpha m_3}{2m_0 - m_1 - m_2}$$

Based on the Curie temperatures estimated from K-T curves, a temperature of 475 °C was used for the different heatings. This temperature is low enough to reduce the risk of thermal alteration of the magnetic mineralogy but sufficient to create a significant partial thermoremanence. Experiments were performed using an ASC Scientific TD48-SC furnace.

A set of laboratory fields ranging from 20 to 70 μT was applied to the different sub-specimens, initiating at 20 μT, and increasing its value until the QDB ratio (Dekkers and Böhnel, 2006) plotted above the horizontal zero value. When possible, the experimental procedure was

Table 2

Summary of flow-mean paleodirections.; n is the number of specimens used for calculation; N is the number of treated samples; Inc inclination; Dec declination; α_{95} , R and k radius of 95% confidence angle and precision parameter of Fisher's (1953) statistics; VGP_{Lat.} and VGP_{Long.} are the paleolatitude and paleolongitude of the virtual geomagnetic poles.

| Flow | Lat °N | Long °E | Dec (°) | Inc (°) | α_{95} (°) | n/N | k | R | VGP _{Lat.} (°) | VGP _{Long.} (°) |
|--------|-----------|------------|------------|------------|----------------------|-----|-----|------|----------------------------|-----------------------------|
| XE_01 | 41.4776 | 43.2804 | 205 | −50.7 | 4.6 | 6/8 | 209 | 5.98 | −67.6 | 331.9 |
| XE_02 | 41.4776 | 43.2802 | 200.4 | −57.1 | 2.8 | 7/8 | 464 | 6.99 | −73.9 | 320.1 |
| XE_03 | 41.4775 | 43.2801 | 205.3 | −55.3 | 4.1 | 7/8 | 218 | 6.97 | −69.5 | 321.0 |
| XE_04 | 41.4774 | 43.2801 | 197.4 | −57.5 | 5.4 | 7/8 | 124 | 6.95 | −76.2 | 321.7 |
| XE_05 | 41.4773 | 43.2800 | 191.6 | −51.7 | 5.8 | 8/8 | 92 | 7.92 | −77.0 | 354.2 |
| XE_06 | 41.4773 | 43.2801 | NA | | | | | | | |
| XE_07 | 41.4772 | 43.2802 | 184.6 | −59.9 | 4.2 | 8/8 | 178 | 7.96 | −86.5 | 323.1 |
| XE_08 | 41.4771 | 43.2802 | 187.5 | −57.4 | 4.4 | 7/8 | 190 | 6.97 | −83.3 | 341.8 |
| XE_09 | 41.4770 | 43.2801 | 192.4 | −54.7 | 5.8 | 8/8 | 92 | 7.92 | −78.5 | 342.0 |
| XE_10 | 41.4771 | 43.2801 | 198.5 | −56 | 8.7 | 5/8 | 78 | 4.95 | −74.8 | 326.2 |
| XE_11 | 41.4470 | 43.2803 | 187.3 | −52.1 | 8 | 7/8 | 57 | 6.9 | −79.5 | 7.3 |
| XE_11B | 41.4470 | 43.2803 | 189.9 | −56.8 | 6 | 8/8 | 87 | 7.92 | −81.3 | 338.1 |
| XE_12 | 41.4766 | 43.2802 | 185.2 | −55 | 3.7 | 8/8 | 223 | 7.97 | −82.8 | 7.2 |
| XE_13 | 41.4765 | 43.2800 | 190.6 | −59.1 | 5.7 | 8/8 | 97 | 7.93 | −81.8 | 321.0 |
| XE_14 | 41.4765 | 43.2798 | 191.4 | −55.2 | 6 | 7/8 | 101 | 6.94 | −79.4 | 342.4 |
| XE_15 | 41.4765 | 43.2798 | 187.2 | −58.4 | 6.8 | 7/7 | 79 | 6.92 | −84.0 | 334.3 |
| XE_16 | 41.4765 | 43.2798 | 188.4 | −61.4 | 4.8 | 7/7 | 159 | 6.96 | −83.7 | 301.0 |
| XE_17 | 41.4767 | 43.2798 | 184.1 | −61 | 2.6 | 8/8 | 438 | 7.98 | −86.9 | 301.3 |
| XE_18 | 41.4768 | 43.2798 | 184.6 | −51.2 | 8.2 | 8/8 | 55 | 6.89 | −79.7 | 20.8 |
| XE_19 | 41.4768 | 43.2798 | 177.6 | −51.7 | 3.5 | 7/8 | 307 | 6.98 | −80.7 | 55.9 |
| XE_20 | 41.4768 | 43.2796 | 179.9 | −57.5 | 5.1 | 7/8 | 141 | 6.96 | −86.6 | 44.6 |
| XE_21 | 41.4767 | 43.2796 | 169.9 | −52.9 | 6 | 7/8 | 101 | 6.94 | −78.7 | 91.5 |

repeated to get an equal number of points below and above the horizontal line. All calculations were performed using the VBA software of [Monster et al. \(2015\)](#). Exceptionally, the entire MSP was repeated at a higher temperature of 525 °C for the sample XE-17 (see the details below).

4. Main results

Most of the studied lava flows exhibited irreversible susceptibility vs temperature behavior during the heating and cooling cycles ([Fig. 3](#)), similar to the Toloshi lava flows ([Goguitchaichvili et al., 2021](#)). Two ferromagnetic phases seem to be present in the third part of the flows (see an example in [Figure 3](#), Sample 95 × 086). A relatively low Curie temperature is observed between 180 and 190 °C, while a High-T phase is detected around 550 °C, which most probably corresponds to some Titanium poor titanomagnetites. The Curie points, determined for the remaining samples range between 558 and 576 °C, which again attest to the presence of almost magnetite phases. The irreversibility, and thus thermal instability observed for the majority of samples, seems to be produced at high temperatures, close to the blocking temperature spectra.

Magnetic treatments permitted the precise determination of flow-mean paleodirections for all cases, except for site XE06 (sample 94X048A in [Fig. 4](#)). The chaotic and unstable demagnetization behavior impeded selecting any linear segment going to the origin. For all other flows, both thermal and alternating field treatments showed great efficiency revealing essentially uni-vectorial component magnetization. Viscous remanence is almost nonexistent or easily removed at the very first steps of the magnetic cleanings. Similar to Toloshi's ([Goguitchaichvili et al., 2021](#)), all Khertvisi lava flows yielded a well-defined reverse polarity magnetization, which is very precisely determined ([Fig. 5](#), [Table 2](#)) judging from the precision parameter values of the Fisher statistics.

The mean direction, involving all accepted flows, is Inc. = −56.1°, Dec = 189.5°, $N = 20$, $\alpha_{95} = 2.3^\circ$, $k = 187$. These directions are close to the Toloshi's mean paleodirections, and both slightly deviate clockwise from the geocentric axial dipole direction and the expected directions recalculated from the stable Eurasia reference paleomagnetic poles ([Besse and Courtillot, 2002](#)). We do not believe that this declination deviation is due to some tectonic movements since the duration of lava

emissions apparently happened during a very short time and thus, the secular variation is most probably not averaged. Secular variation parameters ($S_b = 7.8^\circ$ with upper limit $S_{bu} = 8.5^\circ$ and lower limit $S_{bl} = 7.1^\circ$) calculated through virtual geomagnetic pole scatter ([Cox, 1970](#)) yielded very low values compared to the available models ([Tauxe and Kent, 2004](#)).

As multispecimen paleointensity determinations are concerned ([Fig. 6](#)), the reliability criteria applied for the MSP relied on the two reliability checks provided by the MSP-Tool of [Monster et al. \(2015\)](#): the average alteration parameter (Avg. ε_{alt}) and the difference between the theoretical and experimental intersection with the y axis (Δb), since, as mentioned by [Monster et al. \(2015\)](#), “Alteration, domain-state effects or alignment errors, however, may lead to a different intercept”. An Avg. $\varepsilon_{alt} \leq 20\%$ ([Carvallo et al., 2017](#)) was set in this investigation. Additionally, a negative overprint check, i.e. $\Delta dec (\Delta inc) < 15^\circ$ ([Monster et al., 2015](#)) was required.

Three out of the six analyzed flows (XE-07, XE-12, and XE-19) yielded successful domain state corrected (DSCc, [Monster et al., 2015](#)) paleointensity determinations with values between 23.8 μT and 29.3 μT , which are at least 50% lower than the present-field value. Flows XE-08 and XE-17 failed to accomplish the Δb reliability check, while flow XE-15 produced no reliable results at all. Moreover, flow XE-17 yielded a higher DSCc field value of 56.3 μT . Worth noting is the fact that, despite the low chosen heating temperature of 475 °C, Avg ε_{alt} range is between 8.7 and 22.5%.

We also note that the %NRM lost values for flows XE-15 and XE-17 obtained during the MSP carried out at a temperature of 475 °C were at the most 23% and 34%, respectively; which are likely low enough to be considered as a suitable pTRMs for reliable determination. Therefore, for these two flows, we decided to repeat the entire MSP but at a higher temperature. This approach seems to be adequate since the Avg ε_{alt} obtained for these flows was well below the threshold value of 20%, and all the specimens will experience again the same thermal history. Thus, the entire MSP was repeated for these flows at a temperature of 525 °C. This time, the %NRM lost values obtained for flow XE-17 was 50% on average, and yielded a slightly higher DSCc field value of 59.1 μT , with an Avg ε_{alt} of 9% and fulfilling the reliability criteria established. It is highly encouraging that both measurements yielded very similar values. Again, flow XE-15 failed to provide any reliable paleointensity determination. Detailed results -Min and Max PI values, Δb , and Avg ε_{alt}

Table 3

MSP paleointensity data. Protocol: MSP-DBc, MSP-FCc, and MSP-DSCc: alignment-corrected Dekkers-Bönnel (DB) ratio, fraction corrected (FC) and domain-state corrected (DSC) multispecimen determination, as defined in [Monster et al. \(2015\)](#). PI: paleointensity result. Min and Max: minimum and maximum paleointensity determination bounds. n/N: number of used (n) and the total specimens (N) analyzed for paleointensity determination. ϵ_{alt} : average alteration parameter. Δb : ordinate axis intercept of the linear fit. R^2 : quality of the linear least-squares fit.

| Flow XE07 | | | | | | | |
|-----------|------|------|------|-----|------------------|------------|-------|
| PROTOCOL | PI | Min | Max | n/N | ϵ_{alt} | Δb | R^2 |
| MSP-DBc | 29.6 | N.A. | N.A. | 4/5 | −22.5 | N.A. | 0.987 |
| MSP-FCc | 32.0 | N.A. | N.A. | 4/5 | −22.5 | −0.01 | 0.990 |
| MSP-DSCc | 29.3 | N.A. | N.A. | 4/5 | −22.5 | 0.00 | 0.988 |

| Flow XE08 | | | | | | | |
|-----------|------|------|------|-----|------------------|------------|-------|
| PROTOCOL | PI | Min | Max | n/N | ϵ_{alt} | Δb | R^2 |
| MSP-DBc | 23.8 | 23.2 | 24.0 | 4/5 | −18.6 | N.A. | 0.962 |
| MSP-FCc | 22.6 | 21.5 | 22.0 | 4/5 | −18.6 | −0.25 | 0.953 |
| MSP-DSCc | 18.9 | 17.9 | 18.5 | 4/5 | −18.6 | −0.25 | 0.959 |

| Flow XE12 | | | | | | | |
|-----------|------|------|------|-----|------------------|------------|-------|
| PROTOCOL | PI | Min | Max | n/N | ϵ_{alt} | Δb | R^2 |
| MSP-DBc | 29.6 | 28.3 | 30.8 | 4/4 | −11.7 | N.A. | 0.991 |
| MSP-FCc | 29.3 | 28.1 | 30.5 | 4/4 | −11.7 | −0.07 | 0.995 |
| MSP-DSCc | 24.9 | 23.8 | 25.9 | 4/4 | −11.7 | −0.02 | 0.995 |

| Flow XE17 | | | | | | | |
|-----------|------|------|------|-----|------------------|------------|-------|
| PROTOCOL | PI | Min | Max | n/N | ϵ_{alt} | Δb | R^2 |
| MSP-DBc | 72.1 | 61.9 | N.A. | 3/4 | −8.7 | N.A. | 0.934 |
| MSP-FCc | 71.9 | 65.0 | 78.5 | 3/4 | −8.7 | −0.09 | 0.985 |
| MSP-DSCc | 56.3 | 50.0 | 62.5 | 3/4 | −8.7 | 0.14 | 0.978 |

| Flow XE17 @ 525 °C | | | | | | | |
|--------------------|------|------|------|-----|------------------|------------|-------|
| PROTOCOL | PI | Min | Max | n/N | ϵ_{alt} | Δb | R^2 |
| MSP-DBc | 66.3 | 58.7 | 70.2 | 3/3 | −9.0 | N.A. | 0.975 |
| MSP-FCc | 66.8 | 60.8 | 70.4 | 3/3 | −9.0 | −0.03 | 0.989 |
| MSP-DSCc | 59.1 | 55.4 | 61.6 | 3/3 | −9.0 | −0.04 | 0.996 |

| Flow XE-19 | | | | | | | |
|------------|------|------|------|-----|------------------|------------|-------|
| PROTOCOL | PI | Min | Max | n/N | ϵ_{alt} | Δb | R^2 |
| MSP-DBc | 30.2 | 28.5 | 32.5 | 4/4 | −13.9 | N.A. | 0.975 |
| MSP-FCc | 29.7 | 28.0 | 32.4 | 4/4 | −13.9 | −0.01 | 0.977 |
| MSP-DSCc | 23.8 | 21.0 | 27.0 | 4/4 | −13.9 | 0.10 | 0.957 |

values, including the other ratios (DBc and FCc)- can be consulted in [Table 3](#).

5. Discussion and conclusions

The new isotopic age determinations indicate that the lavas of the Khertvisi section erupted in the Early Pleistocene, at the boundary of the Gelasian and Calabrian ages in a time span of 1.88 to 1.71 Ma; in good agreement with the Toloshi lava sequence (1.93–1.78 Ma). Although a sedimentary layer is observed in both sections, the duration of the lava emissions seems to be very short – unable to average paleosecular variation. All studied lava flows yielded reverse polarity magnetization, while mean paleodirections are slightly deviated (clockwise) from the axial dipole and expected directions. The upper part of the sequence

(few lava flows) above the reddish sedimentary layer may be alternatively correlated to Chron C1r.3r in the geomagnetic polarity time scale, and the lower part (the great majority of lava flows) below the mentioned layer to Chron C2r.1r. This approach suggests that the whole Olduvai subchron is completely missing in both Khertvisi (this study) and Toloshi ([Goguitchaichvili et al., 2021](#)) profiles. However, this alternative correlation is probably untenable because of the following: 1) It appears that most consecutive (sequential) flows of the Khertvisi sequence show undistinguishable palaeomagnetic directions. For this reason, and in order to analyze the characteristics of secular variation recorded in the sequence, several directional groups (DG) may be defined. If the 95% confidence ovals of the directions of two consecutive flows did not overlap, both directions are considered to be different. This procedure was systematically applied (see for instance [Goguitchaichvili et al., 2009](#) and [Caccavari et al., 2014](#)) to the Javakheti lava sequences (see also [Goguitchaichvili et al., 2021](#)). However, in the present case, the scatter of individual VGP directions is extremely low and lavas above and below the reddish sedimentary layer show statistically undistinguishable paleodirections, indicating that all flows were emitted in a very narrow age interval; 2) The Olduvai normal subchron is not uniform and still no consensus exists on the duration and length. This is perfectly illustrated by listing major paleomagnetic and associated geochronology works in [Goguitchaichvili et al., 2021](#). Namely, many previous studies based on high-quality supported isotopic data, persistently reveal reverse polarity short-lived events within the Olduvai subchron.

Besides great efforts during the last few decades, reliable paleointensity data are still insufficient to document a long-term variation in the intensity of the Earth's magnetic field. A major reason for this paucity is that absolute paleointensity is the most difficult component of the geomagnetic field to determine, and the laboratory experiment failure rate is generally 80 or even higher for volcanic rocks. Even though high-quality Thellier paleointensity determinations are obtained, their interpretation in terms of geomagnetic significance is complex ([Calvo et al., 2002](#)). Judging from continuous thermomagnetic curves, it is clear that Khertvisi samples are unsuitable for Thellier double heating paleointensity experiments. In this study, paleointensity determinations were accomplished with the multispecimen parallel differential pTRM method ([Dekkers and Bönnel, 2006](#)), together with the protocols for fraction and domain-state corrections (FC and DSC, respectively) proposed by [Fabian and Leonhardt \(2010\)](#) meeting most strict selection and quality criteria. In this context, five new, technically high-quality determinations should be considered as an absolute success.

[Goguitchaichvili et al. \(2000\)](#) reported a reconnaissance study in three volcanic provinces in Georgia, Kazbegi, Kharmi, and Djavakheti ([Camps et al., 1996](#); [Calvo-Rathert et al., 2008](#) and [2015](#)). This survey also included the new evaluation of previous paleomagnetic results obtained by [Sologashvili \(1986\)](#) in an extensive paleomagnetic and magnetostratigraphic study carried out on more than a hundred lava flows from these three main Pliocene and Quaternary volcanic regions in Georgia. The absolute geomagnetic paleointensities obtained from Georgian volcanic units vary between 16.3 and 54.7 μT . It is worth mentioning that two intermediate-polarity samples yield significantly reduced paleointensities ([Calvo-Rathert et al., 2015](#)). Discarding intermediate polarity sites, a mean value of a virtual dipole moment (VDM) of $7.8 \pm 3.7 \cdot 10^{22} \text{ Am}^2$ is obtained close to the present-day value. [Calvo-Rathert et al. \(2011\)](#) analyzed more than 20 basaltic lava flows belonging to four different profiles in the southern Caucasus. Most flows yielded paleointensity results in the 30–45 μT range, in accordance with expected Pliocene to present-day intensities. Two flows, however, yielded high paleointensity values around 60 μT . [Goguitchaichvili et al. \(2001\)](#) reported many successful Thellier type absolute geomagnetic paleointensity determinations from a Pleistocene lava sequence located in the Lesser Caucasus. Flow-mean Thellier paleointensity values range from 16.3 ± 5.2 to $71.0 \pm 0.3 \mu T$. The lowest values correspond to the

transitional field regime and correspond to the Matuyama-Olduvai polarity transition.

Four flows belonging to the Khertvisi profile yielded paleointensities ranging from 18.9 to 29.3 μT . Generally speaking, these values are close to transitional field intensities reported in Georgia during the Matuyama and Bruhnes chrons. One more Khertvisi flow provided higher paleointensity compared to the present-day field. Considering all these factors together, we definitively do not claim the existence of a transitional (geomagnetic reversal or excursion) field. However, high-quality paleomagnetic and absolute paleointensity data, supported by four isotopic ages and excellent stratigraphic control, most probably permit us to consider the Khertvisi section as the strong volcanic evidence of an unusual geomagnetic regime across the Olduvai subchron.

Author statement

This study is headed by Avto Goguitchaichvili and Juan Morales. All authors actively participated either in field trips, laboratory experiments, interpretation and editing.

Declaration of Competing Interest

We explicitly declare that there is no conflict of interest.

Data availability

Data will be made available on request.

Acknowledgments

This work was funded by project PID2019-105796GB-I00/AEI/10.13039/501100011033 (Spanish Agencia Estatal de Investigación). This study was partially supported by the Natural Sciences and Engineering Research Council of Canada for V.A.K. (NSERC grant RGPIN-2019-04780). AG is grateful to DGAPA-UNAM (Mexico) for the support during the sabbatical at University of Alberta).

References

- Besse, J., Courtillot, V., 2002. Apparent and true polar wander and the geometry of the geomagnetic field over the last 200 Myr. *J. Geophys. Res. Solid Earth* 107 (B11), EPM-6. <https://doi.org/10.1029/2000JB000050>.
- Caccavari, A., et al., 2014. Paleomagnetism of the 40Ar/39Ar age of a Pliocene lava flow sequence in the lesser Caucasus: record of a clockwise rotation and analysis of paleosecular variation. *Geophys. J. Int.* 197, 1354–1370. <https://doi.org/10.1093/gji/ggu097>.
- Calvo, M., Prévot, M., Perrin, M., Riisager, J., 2002. Investigating the reasons for the failure of paleointensity experiments: A study on historical lava flows from Mt. Etna. *Geophys. J. Int.* 149, 44–63.
- Calvo-Rathert, M., Goguitchaichvili, A., Sologashvili, D., Villalain, J.J., Bógalo, M.F., Carrancho, A., Maissuradze, G., 2008. New paleomagnetic data from the hominin bearing Dmanisipaleoanthropologic site (southern Georgia, Caucasus). *Quat. Res.* 69, 91–96.
- Calvo-Rathert, M., Goguitchaichvili, A., Vashakidze, G., Sologashvili, J., et al., 2015. New paleomagnetic and paleointensity data from Georgia (Caucasus): a review. *Latinmag Lett.* 4 (LL15-0503Rv), 1–22.
- Calvo-Rathert, M., Goguitchaichvili, A., Bógalo, M.F., Vegas-Tubía, N., Carrancho, A., Sologashvili, J., 2011. A paleomagnetic and paleointensity study on Pleistocene and Pliocene basaltic flows from the Djavakheti Highland (Southern Georgia, Caucasus). *Phys. Earth Planet. Inter.* 187, 212–224.
- Camps, P., Ruffet, G., Shcherbakov, V.P., Shcherbakova, V.V., Prévot, M., Moussine-Pouchkine, A., Sholpoe, L., Goguitchaichvili, A., Asanidzé, B., 1996. Paleomagnetic and geochronological study of a geomagnetic field reversal or excursion recorded in Pliocene volcanic rocks from Georgia (Lesser Caucasus). *Phys. Earth Planet. Inter.* 96 (1), 41–59. [https://doi.org/10.1016/0031-9201\(95\)03110-3](https://doi.org/10.1016/0031-9201(95)03110-3).
- Carvalho, C., Camps, P., Sager, W.W., Poidras, T., 2017. Palaeointensity determinations and magnetic properties on Eocene rocks from Izu-Bonin-Mariana forearc (IODP Exp. 352). *Geophys. J. Int.* 210, 1993–2009. <https://doi.org/10.1093/gji/ggx208>.
- Channell, J.E.T., Mazaud, A., Sullivan, P., Turner, S., Raymo, M.E., 2002. Geomagnetic excursions and paleointensities in the Matuyama Chron at Ocean Drilling Program sites 983 and 984 (Iceland Basin). *J. Geophys. Res. Solid Earth* 107 (B6), EPM-1. <https://doi.org/10.1002/2016JB013616>.
- Channell, J.E.T., Singer, B.S., Jicha, B.R., 2020. Timing of Quaternary geomagnetic reversals and excursions in volcanic and sedimentary archives. *Quat. Sci. Rev.* 228, 106114. <https://doi.org/10.1016/j.quascirev.2019.106114>.
- Cox, A., 1970. Latitude dependence of the angular dispersion of the geomagnetic field. *Geophys. J. R. Astron. Soc.* 20 (3), 253–269. <https://doi.org/10.1111/j.1365-246X.1970.tb06069.x>.
- Cox, A., Dalrymple, G.B., 1967. Statistical analysis of geomagnetic reversal data and the precision of potassium-argon dating. *J. Geophys. Res.* 72 (10), 2603–2614.
- Cox, A., Doell, R.R., Dalrymple, G.B., 1963. Geomagnetic polarity epochs and Pleistocene geochronometry. *Nature* 198, 1049e1051.
- Dekkers, M.J., Böhm, H.N., 2006. Reliable absolute palaeointensities independent of magnetic domain state. *Earth Planet. Sci. Lett.* 248 (1–2), 508–517. <https://doi.org/10.1016/j.epsl.2006.05.040>.
- Fabian, K., Leonhardt, R., 2010. Multiple-specimen absolute paleointensity determination: an optimal protocol including pTRM normalization, domain-state correction, and alteration test. *Earth Planet. Sci. Lett.* 297 (1–2), 84–94. <https://doi.org/10.1016/j.epsl.2010.06.006>.
- Fisher, R.A., 1953. Dispersion on a sphere. *Proc. Royal Soc. London. Series A. Math. Phys. Sci.* 217 (1130), 295–305. <https://doi.org/10.1098/rspa.1953.0064>.
- Goguitchaichvili, A., Calvo-Rathert, M., Sologashvili, D., Alva Valdivia, L., Urrutia-Fucugauchi, J., 2000. Paleomagnetism of the Georgian Plio-Quaternary Volcanic Provinces (Southern Caucasus): A Pilot Study. *Compt. Rend. Acad. Sci. Paris* 11, 331, 683–690.
- Goguitchaichvili, A., Calvo-Rathert, M., Sologashvili, D., Morales, J., Soler, A.M., Espinosa, M., 2001. A reconnaissance magnetostratigraphy of Georgian Plio-Quaternary Volcanic Provinces (Southern Caucasus). *Geofis. Int.* 40, 111–119.
- Goguitchaichvili, A., Cervantes, M.A., Calvo-Rathert, M., Camps, P., Sologashvili, J., Maissuradze, G., 2009. Gilbert-Gauss geomagnetic reversal recorded in Pliocene volcanic sequences from Georgia (Lesser Caucasus): revisited. *Earth Planets Space* 61 (1), 71–81. <https://doi.org/10.1186/BF03352886>.
- Goguitchaichvili, A., Gómez, B., Rathert, M.C., Lebedev, V., Cervantes, M., Vashakidze, G., Sologashvili, J., Morales, J., 2021. Noise across Olduvai Subchron: Paleomagnetic study of a Pliocene lava succession from Javakheti Highland (Georgia, Lesser Caucasus). *Phys. Earth Planet. Inter.* 311, 106641. <https://doi.org/10.1016/j.pepi.2020.106641>.
- Kirschvink, J., 1980. The least-squares line and plane and analysis of paleomagnetic data. *Geophys. J. Int.* 62 (3), 699–718. <https://doi.org/10.1111/j.1365-246X.1980.tb02601.x>.
- Kusu, C., Okada, M., Nozaki, A., Majima, R., Wada, H., 2016. A record of the upper Olduvai geomagnetic polarity transition from a sediment core in southern Yokohama City, Pacific side of central Japan. *Prog. Earth Planet. Sci.* 3 (1), 1–13. <https://doi.org/10.1186/s40645-016-0104-7>.
- Lebedev, V.A., Bubnov, S.N., Dudauri, O.Z., Vashakidze, G.T., 2008. Geochronology of Pliocene volcanism in the Dzhavakheti Highland (the lesser Caucasus). Part 1: Western part of the Dzhavakheti Highland. *Stratigr. Geol. Correl.* 16 (2), 204–224. <https://doi.org/10.1134/S0869593808020081>.
- Lebedev, V.A., Chernyshev, I.V., Chugaev, A.V., Gol'tsman, Y.V., Bairova, E.D., 2010. Geochronology of eruptions and parental magma sources of Elbrus volcano, the Greater Caucasus: K-Ar and Sr-Nd-Pb isotope data. *Geochim. Int.* 48 (1), 41–67. <https://doi.org/10.1134/S0016702910010039>.
- Lebedev, V.A., Vashakidze, G.T., Parfenov, A.V., Yakushev, A.I., 2019. The origin of adakite-like magmas in the modern continental collision zone: Evidence from Pliocene dacitic volcanism of the Akhalkalaki Lava Plateau (Javakheti Highland, Lesser Caucasus). *Petrology.* 27 (3), 307–327. <https://doi.org/10.1134/S0869591119030056>.
- Lisiecki, L.E., Raymo, M.E., 2005. A Pliocene-Pleistocene stack of 57 globally distributed benthic $\delta^{18}\text{O}$ records. *Paleoceanography* 20 (1). <https://doi.org/10.1029/2004PA001071>.
- Lourens, L.J., Antonarakou, A., Hilgen, F.J., Van Hoof, A.A.M., Vergnaud-Grazzini, C., Zachariasse, W.J., 1996. Evaluation of the Plio-Pleistocene astronomical timescale. *Paleoceanography* 11 (4), 391–413.
- Monster, M.W., De Groot, L.V., Dekkers, M.J., 2015. MSP-Tool: a VBA-based software tool for the analysis of multispecimen paleointensity data. *Front. Earth Sci.* 3, 86. <https://doi.org/10.3389/feart.2015.00086>.
- Ogg, J.G., 2012. Geomagnetic polarity time scale. In: Gradstein, F.M., Ogg, J.G., Schmitz, M., Ogg, G. (Eds.), *The Geologic Time Scale 2012*. Elsevier, p. 85e113.
- Opdyke, M.D., Channell, J.E., 1996. *Magnetic stratigraphy*. Academic press.
- Rivera, T.A., Darata, R., Lippert, P.C., Jicha, B.R., Schmitz, M.D., 2017. The duration of a Yellowstone super-eruption cycle and implications for the age of the Olduvai subchron. *Earth Planet. Sci. Lett.* 479, 377–386. <https://doi.org/10.1016/j.epsl.2017.08.027>.
- Shackleton, N.J., Berger, A., Peltier, W.R., 1990. An alternative astronomical calibration of the lower Pleistocene timescale based on ODP Site 677. *Earth Environ. Sci. Trans. Royal Soc. Edinburgh* 81 (4), 251–261. <https://doi.org/10.1017/S0263593300020782>.
- Singer, B.S., 2014. A Quaternary geomagnetic instability time scale. *Quat. Geochronol.* 21, 29–52. <https://doi.org/10.1016/j.quageo.2013.10.003>.
- Singer, B., Brown, L.L., 2002. The Santa Rosa Event: 40Ar/39Ar and paleomagnetic results from the Valles rhyolite near Jaramillo Creek, Jemez Mountains, New Mexico. *Earth Planet. Sci. Lett.* 197 (1–2), 51–64. [https://doi.org/10.1016/S0012-821X\(01\)00598-2](https://doi.org/10.1016/S0012-821X(01)00598-2).
- Singer, B.S., Laurie, L., 2004. 4 0Ar/3 9Ar chronology of late Pliocene and early Pleistocene geomagnetic and glacial events in southern Argentina. *Geophys. Monograph Series* 145. <https://doi.org/10.1029/145GM13>.
- Singer, B.S., Hoffman, K.A., Chauvin, A., Coe, R.S., Pringle, M.S., 1999. Dating transitionally magnetized lavas of the late Matuyama Chron: Toward a new 40Ar/

- ³⁹Ar timescale of reversals and events. *J. Geophys. Res. Solid Earth* 104 (B1), 679–693. <https://doi.org/10.1029/1998JB900016>.
- Singer, B.S., Hoffman, K.A., Coe, R.S., Brown, L.L., Jicha, B.R., Pringle, M.S., Chauvin, A., 2005. Structural and temporal requirements for geomagnetic field reversal deduced from lava flows. *Nature* 434 (7033), 633–636. <https://doi.org/10.1038/nature03431>.
- Sologashvili, D., 1986. Paleomagnetism of Neogene volcanic formations of Georgia. PhD Thesis. University of Tbilissi (168 pp (in Russian)).
- Steiger, R.H., Jäger, E., 1977. Subcommittee on geochronology: convention on the use of decay constants in geo- and cosmochemistry. *Earth Planet. Sci. Lett.* 36 (3), 359–362. [https://doi.org/10.1016/0012-821X\(77\)90060-7](https://doi.org/10.1016/0012-821X(77)90060-7).
- Tauxe, L., Kent, D.V., 2004. A simplified statistical model for the geomagnetic field and the detection of shallow bias in paleomagnetic inclinations: was the ancient magnetic field dipolar? *Geophysical Monograph Series* 145. Am. Geophys. Union. <https://doi.org/10.1029/145GM08>.
- Tric, E., Laj, C., Jéhanno, C., Valet, J.P., Kissel, C., Mazaud, A., Iaccarino, S., 1991. High-resolution record of the Upper Olduvai transition from Po Valley (Italy) sediments: support for dipolar transition geometry? *Phys. Earth Planet. Inter.* 65 (3–5), 319–336. [https://doi.org/10.1016/0031-9201\(91\)90138-8](https://doi.org/10.1016/0031-9201(91)90138-8).
- Yang, T., Hyodo, M., Yang, Z., Ding, L., Li, H., Fu, J., Mishima, T., 2008. Latest Olduvai short-lived reversal episodes recorded in Chinese loess. *J. Geophys. Res. Solid Earth* 113 (B5). <https://doi.org/10.1029/2007JB005264>.
- Zijderveld, J.D.A., Hilgen, F.J., Langereis, C.G., Verhallen, P.J.J.M., Zachariasse, W.J., 1991. Integrated magnetostratigraphy and biostratigraphy of the upper Pliocene–lower Pleistocene from the Monte Singa and Crotone areas in Calabria, Italy. *Earth Planet. Sci. Lett.* 107 (3–4), 697–714. [https://doi.org/10.1016/0012-821X\(91\)90112-U](https://doi.org/10.1016/0012-821X(91)90112-U).